

## NEW RESULTS IN THE CONTROL OF ROTOR SYNCHRONOUS VIBRATION

Carl R. Knospe  
R. Winston Hope  
Stephen J. Fedigan  
Ronald D. Williams

Center for Magnetic Bearings  
University of Virginia, Charlottesville, Virginia, USA

### ABSTRACT

Rotor unbalance is most often the primary cause of unacceptable vibration in rotating machinery. Over the last decade, researchers have explored different methods of taking advantage of the active nature of magnetic bearings to attenuate unbalance response including both *feedback* and *adaptive open loop* methods. In this paper, the authors examine the performance of a particular adaptive open loop control algorithm known as *convergent control*. The stability and performance robustness properties of this algorithm are examined both theoretically and experimentally and are shown to be quite good. Experimental results also indicate high performance in vibration attenuation, and quick adaptation to changes in the imbalance condition and rotor speed.

### INTRODUCTION

Many authors have investigated methods for reducing the unbalance response of rotating machinery using magnetic bearings [1-5]. The methods employed fall into two categories: feedback methods and open loop (or feedforward) methods. While both methods can be used to greatly reduce the machine unbalance response, the open loop methods have the distinct advantage of not affecting system stability. Thus, the open loop method can be employed on any rotor system and at any operating speed.

The performance of a truly open loop control strategy relies on the accuracy of a pre-computed schedule of control action since this schedule cannot be corrected based upon resulting performance. This accuracy is dependent on (1) *a priori* knowledge of the system

dynamics, and (2) knowledge of future disturbances to the system. The inability to correct an incorrect schedule, can be overcome by re-computing the schedule periodically. If the length of the schedule is much longer than the largest time constant of the system (i.e., closed loop system for magnetic bearings), this adaptive algorithm can still be thought of as a true open loop controller. While this controller could also be viewed as a very slow, nonlinear feedback controller, this paradigm is not very useful in designing such controllers or in analyzing their behavior.

In this paper, an adaptive open loop control algorithm is proposed. A general theoretical framework for the performance of the algorithm is also presented in Section 2. Stability and performance robustness of the algorithm is considered in Section 3. In Section 4, experimental results for the algorithm are obtained from a laboratory test rig using a digital controller. This work builds on that previously presented by the authors in [1].

### ADAPTIVE OPEN LOOP CONTROL: THE CONVERGENT CONTROL ALGORITHM

The concept of the adaptive open loop control is quite simple: synchronous perturbation control signals are generated and added to the feedback control signals so as to cancel rotor synchronous response. These synchronous signals consist of sinusoids that are fixed to the shaft angular position via a keyphasor signal. The magnitude and phase of these sinusoids is periodically adjusted so as to minimize the rotor's unbalance response. These updates occur slowly in comparison to the decay of the rotor's transient response. For this reason, this method can be considered as the adaptation of a set of open loop signals.

The primary issue in employing this method is how to update the magnitude and phase of the open loop signals so as to minimize the synchronous vibration. Any method to be employed should have quick convergence to the minimum vibration, be computationally quick, and should have good stability and performance robustness. Here, we examine a simple algorithm, called *convergent control*, which satisfies these requirements.

The rotor vibration can be related to the applied open loop signals via

$$X = TU + X_0$$

where  $X$  is a  $n$ -vector of the synchronous Fourier coefficients of the  $n/2$  vibration measurements,  $U$  is a  $m$ -vector of the synchronous Fourier coefficients of the  $m/2$  applied open loop signals,  $X_0$  is a  $n$ -vector of the synchronous Fourier coefficients of the uncontrolled vibration, and  $T$  is a  $n \times m$  matrix of influence coefficients relating the open loop signals to the measurements.

Since the open loop algorithm updates the control vector  $U$  periodically, the subscript  $i$  will be used to denote the  $i$ 'th update. The time between the  $i$ 'th and  $i+1$ 'th update is referred to as cycle  $i$  of the algorithm. During cycle  $i$ , the control  $U_i$  is applied resulting in the vibration  $X_i$ . This vibration vector is computed early during cycle  $i$  using the measurements from the position sensors. This vibration vector is related to the cycle  $i$  control vector by

$$X_i = TU_i + X_{0i} \quad (1)$$

where  $T$  is assumed to be changing very slowly and therefore is not subscripted. During cycle  $i$  the next update of the control vector  $U_{i+1}$  must be computed from the information available in cycle  $i$  (i.e.,  $U_i$  and  $X_i$ ). If we assume that the change in  $X_0$  between cycle  $i$  and  $i+1$  is unknown and has zero mean

$$\Delta X_{0i} = X_{0i+1} - X_{0i} \quad E\{\Delta X_{0i}\} = 0$$

then the optimal control vector  $U_{i+1}$  can be found that minimizes the quadratic performance function

$$J = E\{X_{i+1}^T X_{i+1}\}$$

where  $E\{\}$  is the expected value operator. The optimal control law is given by

$$U_{i+1} = U_i + AX_i \quad (2)$$

$$A \equiv -[T^T T]^{-1} T^T$$

The optimal control law is derived by setting the first variation of the performance index with respect to  $U_{i+1}$  equal to zero (see Appendix)

The matrix  $T$  for a particular operating speed can be estimated off-line through either (1) the injection of frequency rich noise when the rotor is supported but not spinning, or (2) the injection of synchronous test forces when the rotor is spinning. The second method, while more time-consuming, will accurately account for the effect of gyroscopics on the influence coefficient matrix. For the rotor considered in Section 4, gyroscopics are not a significant effect and both methods of identification yield good performance.

The off-line identification results in a set of estimated  $T$  matrices  $\{\hat{T}_1, \hat{T}_2, \dots, \hat{T}_k, \dots, \hat{T}_M\}$  associated with a set of operating speeds  $\Omega \equiv \{\omega_1, \omega_2, \dots, \omega_k, \dots, \omega_M\}$  which span the operating speed range. Each of these matrices is then used to compute a gain matrix  $A_k$  for the associated operating speed  $\omega_k$

$$A_k = -[\hat{T}_k^T \hat{T}_k]^{-1} \hat{T}_k^T$$

When the rotor is operating at speed  $\omega$ , the  $A$  matrix used in updating the control vector is determined by an element-wise linear interpolation of the  $A$  matrices for the operating speeds in the set  $\Omega$  immediately above and below  $\omega$

$$A = \left( \frac{\omega_{k+1} - \omega}{\omega_{k+1} - \omega_k} \right) A_k + \left( \frac{\omega - \omega_k}{\omega_{k+1} - \omega_k} \right) A_{k+1} \quad (3)$$

As will be shown later, this interpolation results in better performance than if the  $A$  matrix for the nearest operating speed is used.

#### STABILITY AND PERFORMANCE ROBUSTNESS

The stability and performance robustness of the linear discrete time system governed by Eqns. (1) and (2) can be easily analyzed. Simplifying these two equations yields either

$$X_{i+1} = [I + TA]X_i$$

or

$$U_{i+1} = [I + AT]U_i + AX_{0i}$$

The stability of these equations is obviously governed by the eigenvalues of  $[I+TA]$  and  $[I+AT]$  respectively. For stability, all the eigenvalues must be inside the unit circle in the complex plane. Another way of expressing this, is to require that the 2-norm of  $X_{i+1}$  be less than the 2-norm of  $X_i$ ,

$$\|X_{i+1}\|_2 < \|X_i\|_2$$

or that

$$\bar{\sigma}(I + TA) < 1$$

where  $\bar{\sigma}(\bullet)$  is the maximum singular value. Additionally, the maximum singular value can be used to measure performance. The slowest rate of decay in the magnitude of the vibration vector is given by the maximum singular value of  $[I + TA]$

$$\delta(A, T) \equiv \bar{\sigma}(I + TA)$$

$$\|X_{i+1}\|_2 = \delta(A, T)\|X_i\|_2$$

where  $\delta$  is called the *decrement*. If the matrix  $T$  is square (the number of vibration measurements used is equal to the number of bearing axes), then the vibration vector will converge to zero if the decrement is less than 1. This can be used to prove the following theorems for stability and performance robustness.

### Theorem 1: Stability Robustness to Additive Error in Estimate

If the error in the estimate of  $T$  is given by the additive error matrix  $E_a$

$$T = \hat{T} + E_a$$

then the discrete time system will be stable and the vibration will converge to 0 if

$$\bar{\sigma}(E_a) < \underline{\sigma}(\hat{T})$$

where  $\underline{\sigma}(\bullet)$  is the minimum singular value.

### Theorem 2: Stability Robustness to Multiplicative Error in Estimate

If the error in the estimate of  $T$  is expressed as either a multiplicative input error matrix  $E_m^I$  or a multiplicative output error matrix  $E_m^O$

$$T = \hat{T}[I + E_m^I] \quad \text{or} \quad T = [I + E_m^O]\hat{T}$$

then the discrete time system will be stable and the vibration will converge to zero if

$$\bar{\sigma}(E_m^I) < \frac{1}{\kappa(\hat{T})} \quad \text{or} \quad \bar{\sigma}(E_m^O) < 1$$

where  $\kappa(\bullet)$  is the condition number.

Note that an error in the estimate of a square  $T$  does not degrade the steady state performance of the algorithm if discrete time system stability is maintained; the vibration vector continues to converge to zero. However, the rate of convergence, another performance measure of interest, will be affected.

### Theorem 3: Performance Robustness to Errors in Estimate

For the error matrices described above, the discrete time system vibration will converge to zero with a rate given by the decrement  $\delta$  if any of the following conditions on estimate error are satisfied

$$\bar{\sigma}(E_a) \leq \underline{\sigma}(\hat{T})\delta$$

$$\bar{\sigma}(E_m^I) \leq \frac{1}{\kappa(\hat{T})}\delta$$

$$\bar{\sigma}(E_m^O) \leq \delta$$

The above theorems can be extended to treat non-square  $T$  matrices. In this case, however, convergence may not result in the minimum possible value of the performance index.

## EXPERIMENTAL RESULTS

A laboratory test rig with 2 radial magnetic bearings was used to demonstrate the adaptive open loop algorithms using a high-speed, multi-tasking digital controller. The rotor of this rig has a 12.7 mm (0.5 inch) diameter and a 508 mm (20 inches) bearing span. Eddy current position sensors are located vertically and horizontally 32 mm (1.25 inch) outboard from the center of each bearing and 51 mm (2 inches) inboard from the center of the mid

span disk. The first three critical speeds of this machine are at 2700, 4200, and 5500 rpm. Vibration readings from all six sensors were used by the adaptive open loop algorithm.

The convergent control algorithm described in the previous section was implemented on a digital controller designed and built at the University of Virginia's Center for Magnetic Bearings [6]. The digital controller is a 32 bit floating point machine using a Texas Instruments TMS320C30 digital signal processor. The control algorithms were executed under a multi-tasking real time operating system written at the University [7]. One cycle of the adaptive open loop process requires approximately 0.2 seconds to execute.

In the first experiment performed, the influence coefficient matrices were estimated from synchronous current injections at 2200 rpm. The robustness of the algorithm to errors in  $T$  due to changes in operating speed was then tested in the following manner. With the discrete time gain matrix  $A$  set to the optimal value for 2200 rpm ( $A_{2200}$ ), the convergent algorithm was started at several operating speeds. An experimental value of the decrement for each speed  $\omega$  was computed by taking the ratio of the magnitude of the vibration vector after the first update to that of the uncontrolled vibration. Note that this is a lower bound on the theoretical decrement  $\delta(A_{2200}, T_\omega)$  since the uncontrolled vibration vector will, in general, not be directed in the worst possible direction in the vector space.

This same procedure was used to compute the performance robustness to changes in operating speed for a  $T$  matrix learned at 2700 rpm. The experimental decrements for  $A_{2200}$  and  $A_{2700}$  are shown in Figure 1. Note that the convergence rate decreases (increasing decrement) more rapidly with a change in operating speed for the  $A_{2700}$  controller than for  $A_{2200}$ . This occurs because the  $T$  matrix changes rapidly with speed near the first critical, 2700 rpm. From the figure, it can be seen that the adaptation process is unstable for the  $A_{2200}$  controller if the operating speed is greater than 2500 rpm. Similarly for the  $A_{2700}$  controller the adaptation process is unstable if the operating speed is less than 2600 rpm.

Employing the linear interpolation given by Eqn. (3) to generate the  $A$  matrix using  $A_{2200}$  and  $A_{2700}$  for operating speeds between 2200 and 2700 rpm yields the third decrement curve shown in Figure 1. Notice that the

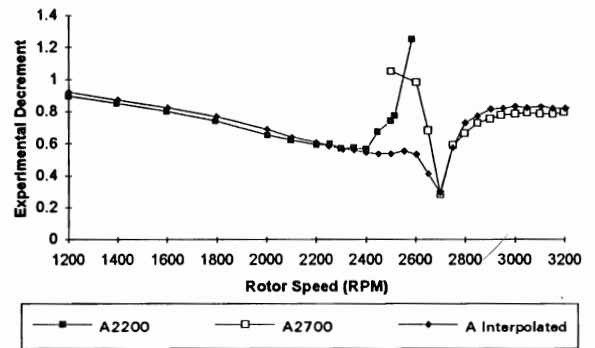


FIGURE 1: Experimental decrement vs. speed

linear interpolation provides a substantially lower decrement (quicker vibration suppression) from 2400 to 2600 rpm than either  $A_{2200}$  or  $A_{2700}$ . From these results it is clear that a look-up table of influence coefficient matrices and linear interpolation between matrices can robustify the adaptive open loop algorithm to changes in speed and substantially improve its rate of convergence.

The performance of the adaptive open loop algorithm over the operating speed range is now examined. Figure 2 shows the baseline performance, the vibration magnitudes at the midspan, inboard, and outboard sensors during a run-up from 1500 to 5000 rpm. As shown in Figure 3, the rotor vibration was substantially reduced when the 30 second run-up was repeated using adaptive open loop control with  $T$  matrices learned via noise injection at frequencies corresponding to every 100 rpm. Note that with this control, it is difficult to detect the rotor's critical speeds as they are passed. Vibration at any particular sensor could be almost completely canceled if this signals were weighted more heavily than others in the quadratic performance index [1].

Figures 4 show the maximum total (feedback plus open loop) synchronous current for the inboard bearing during the run-up with and without adaptive open loop control. Figure 5 shows a similar set of curves for the outboard bearing. As these figures illustrate, the benefits in vibration control demonstrated in Figure 2 have been achieved with a very minor cost in actuator effort. The total synchronous current has increased slightly over only part of the speed range. In fact, over a portion of the operating speed range, both vibration and synchronous bearing current have been reduced.

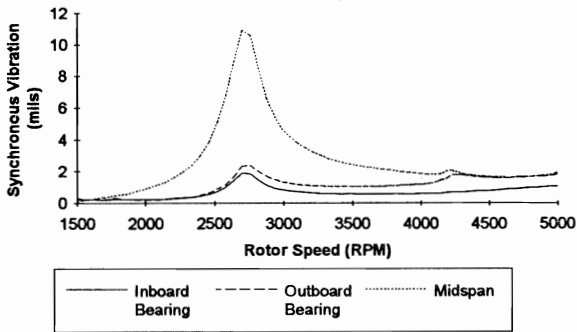


FIGURE 2: Vibration over operating speed range

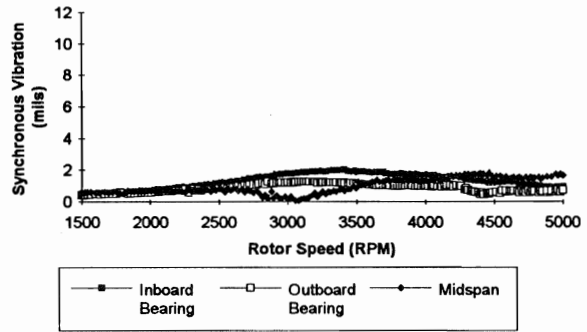


FIGURE 3: Vibration with adaptive open loop control

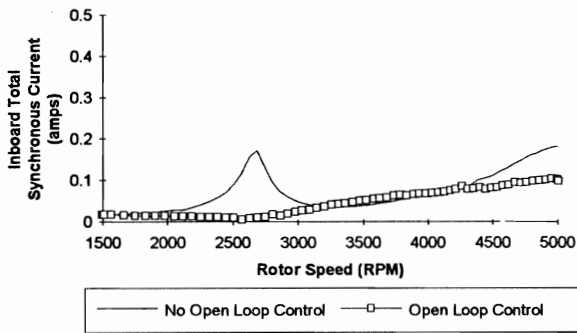


FIGURE 4: Inboard current during run-up

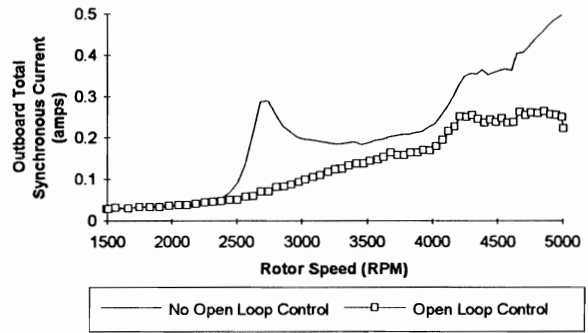


FIGURE 5: Outboard current during run-up

The response of the adaptive open loop controller to a sudden change in unbalance was also tested. The change in rotor imbalance was simulated on the test rig by the addition of unknown synchronous perturbation currents to the control signals. Figure 6 shows the uncontrolled vibration at the midspan sensor during the simulated change in unbalance. The rotor was operating at 2200 rpm. Figure 7 shows the midspan vibration during the same test with the open loop control. Note that the synchronous vibration is nearly completely canceled before the change in unbalance. The adaptive open loop controller requires approximately 0.3 seconds after the change to bring the rotor back to the balanced condition. (The residual vibration shown consists of harmonics of the running speed.)

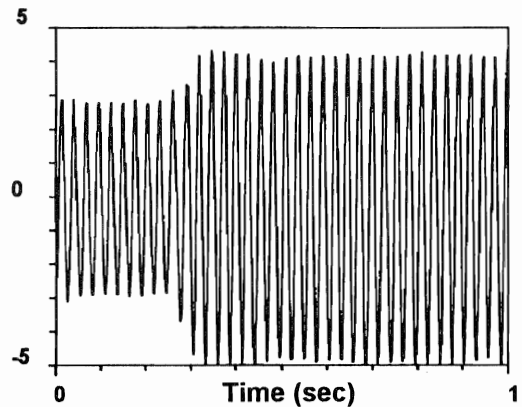


FIGURE 6: Vibration during change in unbalance without open loop control.

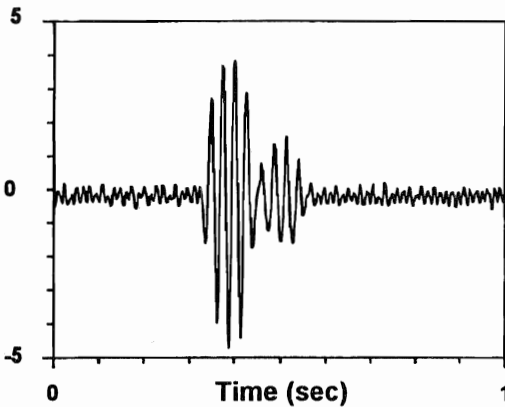


FIGURE 7: Vibration with adaptive open loop control during change in unbalance.

#### SUMMARY

The new theoretical and experimental results presented in this paper clearly indicate the efficacy and robustness of the convergent control algorithm in attenuating machine synchronous vibration. These adaptive open loop control methods are ready to be employed on industrial machines with digital controllers.

#### REFERENCES

1. Knope, C.R., Hope, R.W., Fedigan, S.J., and Williams, R.D. *Adaptive On-Line Rotor Balancing Using Digital Control*. Proceedings of MAG '93 Magnetic Bearings, Magnetic Drives, and Dry Gas Seals Conference and Exhibition, Alexandria, VA, Technomics Publishing, Lancaster, PA, July 1993, pp 153-164.
2. Haberman, H. and Brunet, M. *The Active Magnetic Bearing Enables Optimum Damping of Flexible Rotors*, ASME Paper 84-GT-117, 1984.
3. Burrows, C. and Sahinkaya, M. *Vibration Control of Multi-Mode Rotor-Bearing Systems*. Proceedings of the Royal Society-London, Vol. 386, 1983, p.p. 77-94.
4. Higuchi, T., Otsuk, M., Mizuno, T., and Ide, T. *Application of Periodic Learning Control with Inverse Transfer Function Compensation in Totally Active Magnetic Bearings*. 2nd International Symposium on Magnetic Bearings, Tokyo, Japan, July, 1990, pp. 257-264.
5. Knope, C.R., Humphris, R.R., Maslen, E.H., and Allaire, P.E., 1992 *Active Balancing of a High Speed Rotor in Magnetic Bearings*. Rotordynamics '92, International Conference on Rotating Machine Dynamics, Venice, Italy, April 28-30, Springer-Verlag.

6. Daddio, J.K. *An Integrated Magnetic Bearing Controller*, M.S. Thesis, University of Virginia, May 1992.
7. Fedigan, S.J. *A Real-Time Operating System for a Magnetic Bearing Digital Controller*. M.S. Thesis, University of Virginia, May 1993.
8. Knope, C.R. *Adaptive Control of Systems with Periodic Dynamics*, Ph.D. Dissertation, University of Virginia, May 1989.

#### APPENDIX: DERIVATION OF OPTIMAL CONTROL LAW

For the performance index given, then substitution of Eqns. (1) yields

$$\begin{aligned} J &= E\left\{(TU_{i+1} + X_{0i+1})^T (TU_{i+1} + X_{0i+1})\right\} \\ &= E\left\{(TU_{i+1} + X_{0i} + \Delta X_{0i})^T (TU_{i+1} + X_{0i} + \Delta X_{0i})\right\} \\ &= E\left\{(TU_{i+1} + X_i - TU_i + \Delta X_{0i})^T (TU_{i+1} + X_i - TU_i + \Delta X_{0i})\right\} \end{aligned}$$

Assuming  $T$  is known, this can be simplified to

$$\begin{aligned} J &= U_{i+1}^T T^T TU_{i+1} + U_{i+1}^T T^T X_i - U_{i+1}^T T^T TU_i + U_{i+1}^T T^T E\{\Delta X_{0i}\} \\ &\quad + \{\text{terms not including } U_{i+1}^T\} \end{aligned}$$

(The certainty-equivalent controller is derived here; uncertainty in  $T$  can be included in the derivation yielding the *cautious* controller - see [8] for details)

Taking the first variation of  $J$  with respect to  $U_{i+1}^T$  and setting this equal to zero yields

$$\begin{aligned} 0 &= T^T TU_{i+1} + T^T X_i - T^T TU_i \\ &\quad + T^T E\{\Delta X_{0i}\} \end{aligned}$$

Now, solving for  $U_{i+1}$  gives the optimal control law

$$U_{i+1} = U_i - [T^T T]^{-1} T^T [X_i + E\{\Delta X_{0i}\}]$$

If the expected value of the change in uncontrolled vibration is zero, this simplifies to Eqn. (2).